Int. J. Electrochem. Sci., 14 **(2019)** 11019 – 11034, doi: 10.20964/2019.12.81

International Journal of
ELECTROCHEMICAL
SCIENCE
www.electrochemsci.org

Polyoxometalate Modified Carbon Supported Pd-Cu Bimetallic Catalyst For Formic Acid Oxidation

Zhiwei Zhu[1,2], Chenxi Lu[1,2], Jianzhi Wang[1,2], Xiaoxiao Zhang[1,2], Ning Cai[1,2], Yanan Xue[1,2], Weimin Chen[1,2], Zhiguo Yan[1,2], Xiaojun Yang[1,2], Faquan Yu[1,2], Wei Yang [1,3,], Qifeng Tian [1,2,*]*

[1] Key Laboratory of Green Chemical Process of Ministry of Education & Hubei Key Laboratory of Novel Reactor and Green Chemical Technology (Wuhan Institute of Technology), Wuhan 430205, PR China
[2] School of Chemical Engineering and Pharmacy, Wuhan Institute of Technology, Wuhan 430205, PR China
[3] School of Chemistry and Environmental Engineering, Wuhan Institute of Technology, Wuhan 430205, PR China
[*]E-mail: qftian@wit.edu.cn (Q. T.), yangweight@126.com (W. Y.)

Received: 5 August 2019 / *Accepted:* 5 October 2019 / *Published:* 29 October 2019

Palladium-copper (PdCu) bimetallic alloy nanoparticles were loaded on the polyoxometalate modified carbon supports (PWA-C) to prepare Pd_xCu_y/PWA-C catalyst with different Pd/Cu atomic ratios. Highly dispersion catalyst nanoparticles were obtained and its average particle sizes are in the range of 2.75–4.46 nm. Electrochemical measurements indicated that the formic acid electro-oxidation activities of Pd_xCu_y/PWA-C catalysts were greatly enhanced than the home made Pd/C catalyst. The prepared Pd_xCu_y/PWA-C bimetallic catalyst performed superior electrocatalytic activity and stability than Pd/C catalyst. Among them, Pd_1Cu_2/PWA-C holds the best catalytic performances, whose catalytic activity for formic acid oxidation was improved with a factor of 7.07 as compared to Pd/C catalyst. The outstanding electrocatalytic activity and stability of Pd_xCu_y/PWA-C catalyst may be attributed to the several effects, which include the smaller catalyst nanoparticle, Pd active sites restoring by PWA modification and Cu alloying.

Keywords: Formic acid oxidation, PdCu bimetallic alloy, Electrocatalysis

1. INTRODUCTION

Direct formic acid fuel cell (DFAFC) is a promising power source compared to direct alcohol fuel cell (DAFC) due to its high open circuit potential, low operating temperature, incombustible fuel, safe storage and transportation. These advantages make DFAFC more suitable than DAFC for application in portable electronic devices. Conventionally, the formic acid catalysts apply to formic acid

oxidation (FAO) and converts the chemical energy stored in formic acid into electric energy. However, the Pt catalyst developed for FAO is prone to CO poisoning due to the strong combination of CO and Pt-CO formed in the dehydration of formic acid[1]. Previous studies have shown that the accumulation of CO on Pd surface is slower than that of Pt. Therefore, Pd is more promising than Pt in electrocatalytic oxidation of formic acid[2-5].

Due to the catalytic effect of these nanoparticles (NP) in various chemical reactions, the synthesis of Pd nanoparticles with transition metals and their alloys has attracted a lot of attention. Alloying Pd with other elements not only decrease the amount of Pd in electrocatalysts but also modify the crystallographic and electronic structures of Pd, which may modulate the binding energies between Pd and reactant molecules or the adsorption energies between Pd and reactive intermediates generated in the electro-chemical reaction. The bimetallic alloys of Pd with early transition metal such as Co[6, 7], Ni[8], Ag[9], Cu[10, 11] were reported in fuel cell application. Among above alloyed metals, Pd-Cu catalysts have unique reactivity and selectivity and are widely used in catalytic materials. In addition to develop the new catalyst system, modified carbon supports also play an important role in increasing catalyst activity. Polyoxometalate (POM) are caged structure composed of heteropoly anions and hydrogen ions. A notable and striking feature of Keggin POM is that they can acquire several electrons per molecule without changing the structure. In addition, the reduced morphology retains structure when it is re-oxidized. In other words, they are stable to repeated redox cycles[12]. The phosphotungstic acid (PWA) and phosphomolybdic acid (PMA) are typical polyoxometalate, which contains unique composition of heteropolyanions and countercations. Herring[13] reported that has been achieved through using covalently attached POM moieties as both the proton conducting acid and the radical decomposition catalyst. Previous study has confirmed the synergistic effect between PWA (PMA) and Pd in the Pd/PWA-C[14] and Pd/PMA-PWA-C catalysts[15], respectively. The above research shows that PWA modification can promote electro-oxidation of small organic molecules, such as formic acid.

In this paper, Pd-Cu bimetallic alloys with various Pd:Cu molar ratios are fabricated on PWA modified carbon (Pd_xCu_y/PWA-C, where x:y=2:1, 1:1, 1:2) for formic acid oxidation. XPS is used to structurally characterize the as-synthesized Pd_xCu_y catalysts along with TEM, SEM, XRD, FT-IR, and Raman characterization. The electrocatalytic activity and durability of thus-obtained Pd_xCu_y catalysts are evaluated and compared to those without PWA modification by cyclic voltammetry and chronoamperometry. The effects of PdCu alloying and PWA modification on the supported Pd/C catalysts were investigated and correlated to their catalytic activities of formic acid oxidation.

2. EXPERIMENTAL DETAILS

2.1 Materials and Reagents.

Vulcan XC-72 carbon black, used as catalyst support, was obtained from Cabot Company (USA). $PdCl_2$, $CuCl_2 \cdot 2H_2O$ and PWA were purchased from Sinopharm Chemical Reagent Co. Ltd. (China). All other reagents were used as received without further treatment.

2.2 Preparation of catalysts.

1 g Vulcan XC-72 carbon was added to 50 mL of 3.0×10^{-4} mol L^{-1} PWA solution and stirred in a water bath at 80 ℃ for 12 h. After filtered and washed with ultrapure water, it was dried in vacuum at 60 ℃ for 12 h. After that the composite support PWA-C was obtained. The $NaBH_4$ reduction method were used to synthesized the catalysts. In a typical synthesis of Pd_1Cu_2/PWA-C catalyst, 0.08 g of PWA-C, 20 mL H_2O and 0.064 g $CuCl_2\cdot2H_2O$ was immersed to flask, followed by adding 3.76 mL of 0.05 mol L^{-1} $PdCl_2$ solution to the flask with sonication for 40 min. After it was stirred for 12 h, the mixture was treated in alkaline solution by adding 1 mol L^{-1} Na_2CO_3 until the pH value of the above solution reached 8-9. A freshly prepared $NaBH_4$ was added dropwise afterwards. The product was obtained after the filter residue was washed and dried in a vacuum oven at 60 ℃ for 4 h. The Pd_1Cu_1/PWA-C and Pd_2Cu_1/PWA-C catalysts were obtained in the same process with different amounts of $CuCl_2\cdot2H_2O$. The Pd_1Cu_2/C, Pd_1Cu_1/C and Pd_2Cu_1/C catalyst was prepared according to above procedure except without PWA modification. The Pd loading of each catalyst is 20 wt.%.

2.3 Material characterizations.

The X-ray diffraction (XRD) patterns were recorded on a Bruker D8 Advance Powder X-ray diffractometer using Cu Kα radiation. Surface morphology of sample was characterized by a scanning electron microscope (SEM, ZEISSGeminiSEM500) equipped with an energy dispersive spectroscopy detector (EDS) and transmission electron microscope (TEM, JEM-2100F). X-ray photoelectron spectra (XPS) measurements were conducted using a VG Multilab 2000 spectrometer (Thermo Fisher, USA). IR spectra were recorded on a Thermo ScientificNICOLET 6700 spectrometer (Thermo, USA). Raman spectra (DXR Raman Spectrometer, Thermo, USA) was used to characterize the structure of carbon support.

2.4 Electrochemical measurements.

The electrochemical measurements were carried out using a CHI660E (CH instrument Co., Ltd., China) electrochemical work station with a three-electrode cell. The counter electrode was platinum wire and a saturated calomel electrode (SCE) was a reference electrode. All potentials reported in this paper were referred to the SCE. The glassy carbon electrode (GCE, Φ3) served as working electrode. In a typical electrochemical test, 5.0 mg of sample was dispersed in alcohol containing 0.5 wt.% Nafion solution with 30 min of sonification. A 4.0 μL of dispersed solution was pipetted onto a polished glassy carbon electrode and dried at room temperature. The calculated mass of Pd on the electrode surface is ca. 113 μg cm^{-2}.

For CO stripping measurement, the working electrode was purged with bubbling CO (>99.9% purity) in 0.5 M H_2SO_4 for 30 min at 0.2 V. The dissolved CO was removed by bubbling N_2 for 30 min, after which the CO-stripping voltammograms were recorded by scanning the potential at 50 mV s^{-1}. Cyclic voltammetry of catalysts were conducted over the range of -0.2 to 0.8 V with a scanning rate of

50 mV s^{-1} in the 0.5 M H_2SO_4 + 0.5 M HCOOH mixed solution. Sample stability were also tested by chronoamperometry at constant potential of 0.1 V in the 0.5 M H_2SO_4 + 0.5 M HCOOH mixed solution.

3. RESULTS AND DISCUSSION

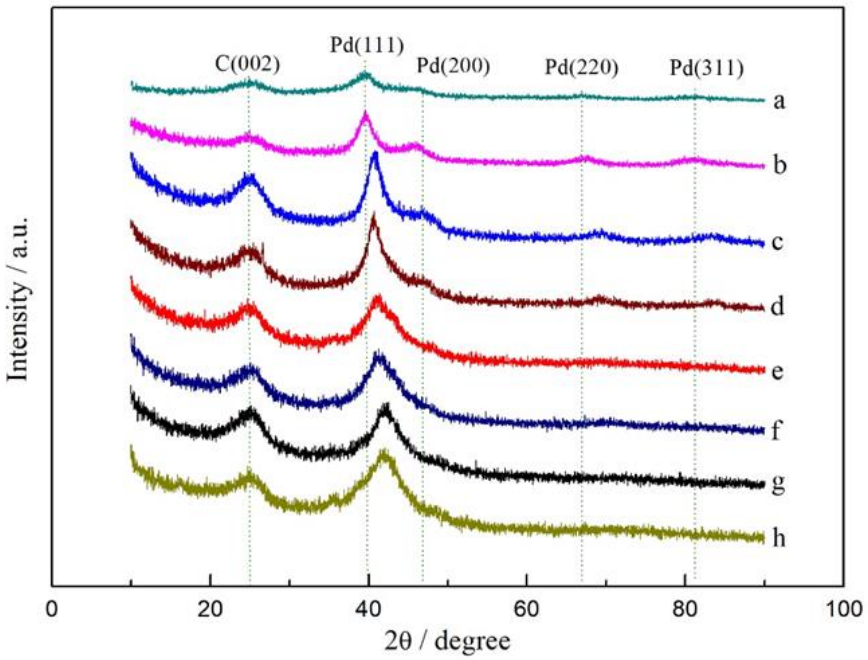

Figure 1. XRD patterns of Pd/PWA-C(a), Pd/C(b), Pd_2Cu_1/PWA-C(c), Pd_2Cu_1/C(d), Pd_1Cu_1/PWA-C(e), Pd_1Cu_1/C(f), Pd_1Cu_2/PWA-C(g), Pd_1Cu_2/C (h) catalysts.

The XRD patterns of Pd/PWA-C, Pd/C, Pd_xCu_y/PWA-C, Pd_xCu_y/C catalysts (x:y=2:1, 1:1, 1:2) are shown in Figure 1. The Pd (111), Pd (200), Pd (220) and Pd (311) peaks appeared in all samples. And their 2θ angles are around 40.1°,46.2°,67.4° and 84.8°, respectively. For the XRD patterns of Pd_xCu_y/PWA-C and Pd_xCu_y/C series catalysts (x:y=2:1, 1:1, 1:2), the diffraction peaks of Pd (111) shifted to higher 2θ angles with increasing Cu content. Similar shift in 2θ angles for PdCu alloy was found by others in the prepared Pd-Cu nanoalloy[16, 17]. Such a shift reflects the contraction of the Pd face center cubic crystalline lattices caused by the partial replacement of Pd atoms with smaller sized Cu atoms. However, there is no significant shift between the PWA modified catalysts and the unmodified ones with the same Pd:Cu atom ratio, which indicates the PWA modification did not change the crystallographic structure of Pd, which is consistent with our previous study[18].

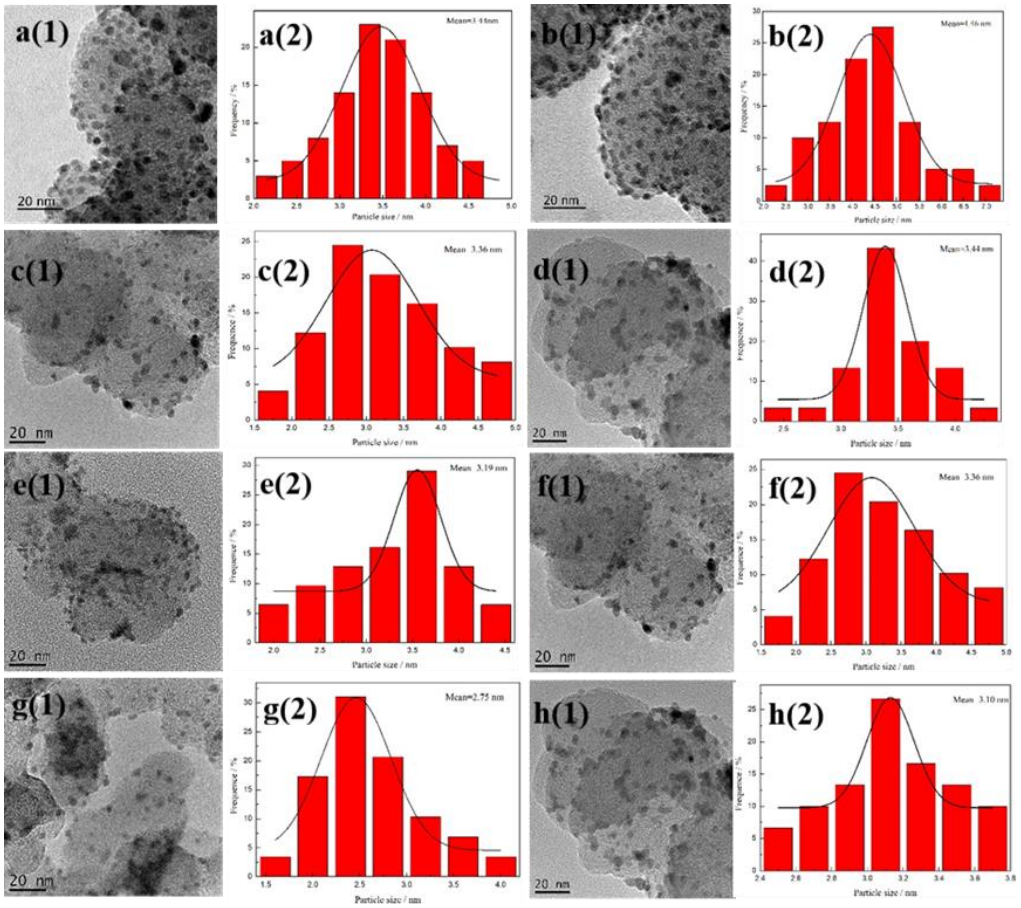

Figure 2. TEM photographs and particle size histograms of the eight catalysts, Pd/PWA-C (a1and a2), Pd/C (b1and b2), Pd_2Cu_1/PWA-C (c1 and c2), Pd_2Cu_1/C (d1 and d2), Pd_1Cu_1/PWA-C (e1 and e2), Pd_1Cu_1/C (f1 and f2), Pd_1Cu_2/PWA-C (g1 and g2), Pd_1Cu_2/C (h1 and h2).

The size and morphology of Pd/PWA-C, Pd/C, Pd_xCu_y/PWA-C, Pd_xCu_y/C catalysts (x:y=2:1, 1:1, 1:2) were observed by TEM in Figure 2. The TEM analyses indicated the catalyst particles of the Pd/PWA-C, Pd/C, Pd_2Cu_1/PWA-C, Pd_2Cu_1/C, Pd_1Cu_1/PWA-C, Pd_1Cu_1/C, Pd_1Cu_2/PWA-C and Pd_1Cu_2/C were spherical with an average diameter of 3.44, 4.46, 3.36, 3.44, 3.19, 3.36, 2.75 and 3.10 nm, respectively. As shown in Figure 2, the Pd_1Cu_2/PWA-C catalyst holds the smallest Pd particle size among the eight catalysts. Furthermore, the average particle size of the Pd_xCu_y/PWA-C catalysts is smaller than the Pd_xCu_y/C catalysts, and the latter also has a smaller particle size than the Pd/C catalyst, which suggests the electrostatic repulsive interactions between the Pd and POM anions weakened agglomeration of the particles. Furthermore, the lattice strain of Pd caused the smaller grain size of catalyst.[15]

Because the electronic structure of the alloy can be changed by lattice strain and charge transfer between the two metals, proper alloying can lead to the narrowing or broadening of d band and the deviation of d band center from Femi level[19, 20]. XPS was performed to identify the atomic valence change of PdCu bimetallic alloy. As shown in Figure 3, the XPS spectra of Pd and Cu in Pd_xCu_y/PWA-C and Pd_xCu_y/C were deconvoluted into two pairs of peaks, respectively. The two peaks at 335.50 and 340.59 eV were attributed to binding energy (BE) of $Pd^0 3d_{5/2}$ and $Pd^0 3d_{3/2}$, respectively. As the Pd on

surface of the catalyst is easily oxidized by the environment[21], the others located at 337.92 and 342.82 eV were attributed to the BE of $Pd^{II}3d_{5/2}$ and $Pd^{II}3d_{3/2}$, respectively.

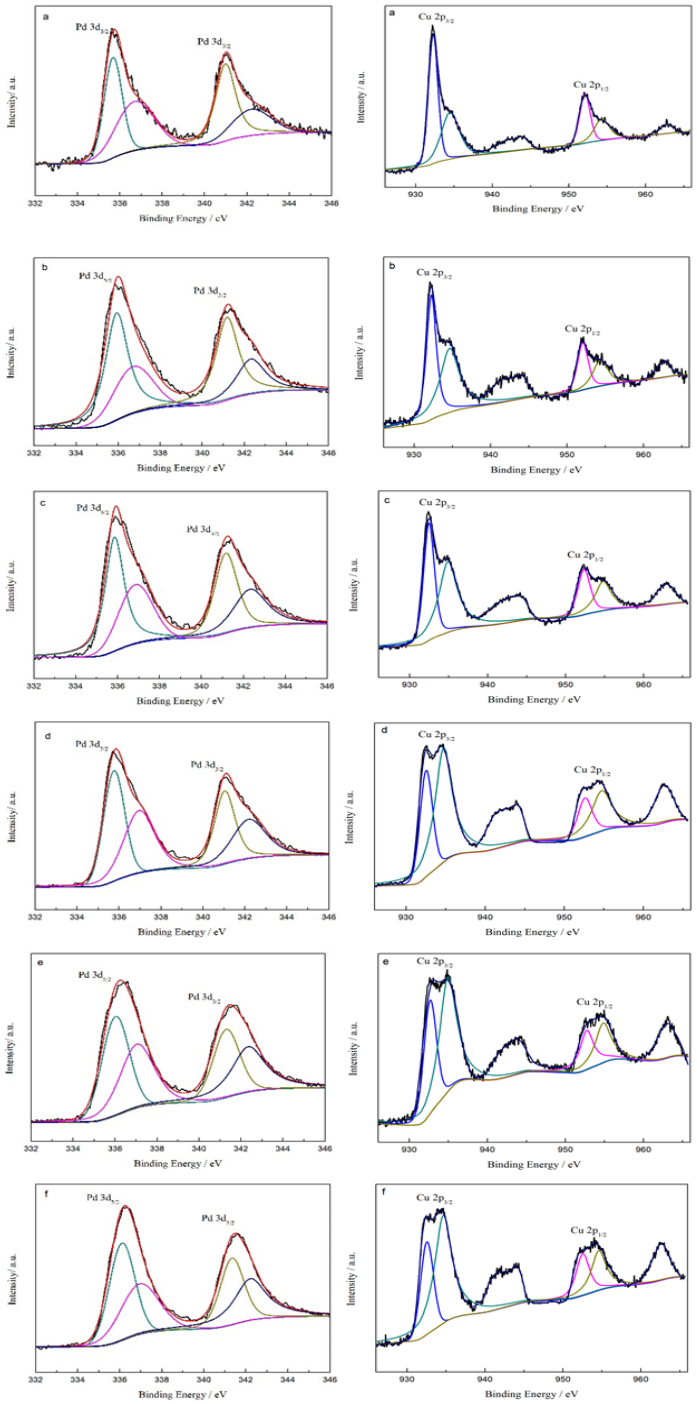

Figure 3. XPS spectra of Pd 3*d* region and Cu 2*p* region for the Pd_1Cu_2/PWA-C(a), Pd_1Cu_1/PWA-C(b), Pd_2Cu_1PWA-C(c) and Pd_1Cu_2/C(d), Pd_1Cu_1/C(e), Pd_2Cu_1/C(f) catalysts.

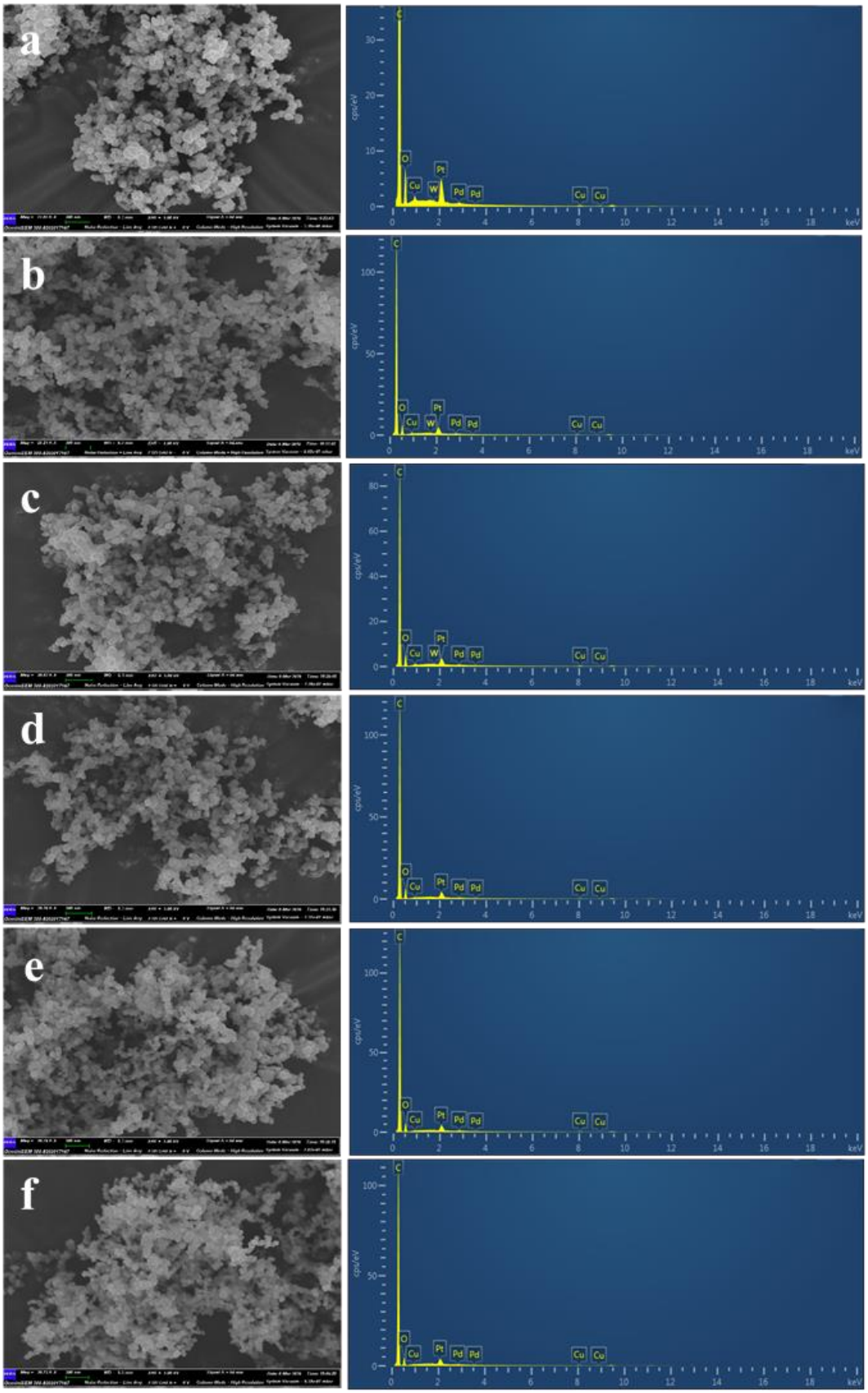

Figure 4. SEM images and EDS spectra of the Pd_1Cu_2/PWA-C(a), Pd_1Cu_1/PWA-C(b), Pd_2Cu_1PWA-C(c) and Pd_1Cu_2/C(d), Pd_1Cu_1/C(e), Pd_2Cu_1/C(f) catalysts.

Table I. Binding Energy (BE)and its shift of Pd 3*d* and Cu 2*p* spectra of Pd/C, Pd/PWA-C, Pd_1Cu_2/PWA-C, Pd_1Cu_1/PWA-C, Pd_2Cu_1/PWA-C and Pd_1Cu_2/C, Pd_1Cu_1/C, Pd_2Cu_1/C catalysts.

Catalysts	Species	Binding Energy （eV）	BE Shift （eV）
Pd/C	$Pd^0 3d_{3/2}$	340.59	0.20
	$Pd^0 3d_{5/2}$	335.40	-0.10
Pd/PWA-C	$Pd^0 3d_{3/2}$	341.12	0.82
	$Pd^0 3d_{5/2}$	335.78	0.28
Pd_1Cu_2/PWA-C	$Pd^0 3d_{3/2}$	341.75	1.45
	$Pd^0 3d_{5/2}$	336.60	1.10
Pd_1Cu_1/PWA-C	$Pd^0 3d_{3/2}$	341.60	1.30
	$Pd^0 3d_{5/2}$	336.35	0.85
Pd_2Cu_1/PWA-C	$Pd^0 3d_{3/2}$	341.40	1.10
	$Pd^0 3d_{5/2}$	336.25	0.75
Pd_1Cu_2/C	$Pd^0 3d_{3/2}$	341.10	0.80
	$Pd^0 3d_{5/2}$	335.90	0.40
Pd_1Cu_1/C	$Pd^0 3d_{3/2}$	341.35	1.05
	$Pd^0 3d_{5/2}$	335.85	0.35
Pd_2Cu_1/C	$Pd^0 3d_{3/2}$	341.05	0.75
	$Pd^0 3d_{5/2}$	335.80	0.30
Pd_1Cu_2/PWA-C	$Cu^0 2p_{3/2}$	932.00	-1.00
Pd_1Cu_1/PWA-C	$Cu^0 2p_{3/2}$	932.25	-0.75
Pd_2Cu_1/PWA-C	$Cu^0 2p_{3/2}$	932.45	-0.65
Pd_1Cu_2/C	$Cu^0 2p_{3/2}$	932.40	-0.60
Pd_1Cu_1/C	$Cu^0 2p_{3/2}$	932.50	-0.50
Pd_2Cu_1/C	$Cu^0 2p_{3/2}$	932.75	-0.25

The BE and its shift of Pd 3*d* and Cu 2*p* spectra for each catalysts is listed in Table I. Compared with the BE of Pd/PWA-C catalyst as studied before,[18] the BE of $Pd^0 3d_{5/2}$ species of Pd_2Cu_1/PWA-C (336.25 eV), Pd_1Cu_1/PWA-C (336.35 eV), Pd_1Cu_2/PWA-C (336.60 eV) catalysts reveal a shift to higher BE with increasing Cu content, which might be related to partial electron transfer from Cu to Pd, as inferred in a detailed discussion on XPS results of Pt–Co and Pt–Ru nanoalloy[22-26]. The positive shift of BE can be attributed to the decrease of adsorption energy of intermediates, thus exposing the active sites on Pd[24]. XPS of Cu 2*p* could be assigned to two sets of peaks. The peaks at 933.00 and 951.62 eV are attributed to $Cu^0 2p_{3/2}$ and $Cu^0 2p_{1/2}$, respectively. The other peaks located at 934.02 and 954.22 eV could be fitted into $Cu^{II} 2p_{3/2}$ and $Cu^{II} 2p_{1/2}$, respectively. The XPS shaking spectra of the satellites in Cu 2*p* region was associated with its oxides. Cu oxides oxygen containing species can react with CO-type intermediate species, resulting the releases of active sites on Pd[27, 28]. The weak peaks of Cu in Pd_xCu_y/C and Pd_xCu_y/PWA-C indicate that the Cu component in the alloy is dominated by the zero-valence state, which confirms the strong oxidation resistance of Cu during Pd alloying. The charge transfer effect contributes to a lowered d-band center as proposed by previous studies[22, 29]. In addition, as confirmed by XRD patterns, alloying Pd with Cu would lead to the contracted lattice

parameter, which also contributed to the narrowed d-band center of Pd, as reported in previous studies on Pt-Co and Pt-Ru[23-25]. The decrease in the center of the d-band of Pd weakens the binding energy between the active center and certain reaction intermediates[30-32], thereby increasing their resistance to toxicity and improving their electrocatalytic properties. Furthermore, the Pd_xCu_y/PWA-C catalyst displayed a higher BE shift compared with the same atomic ratio in Pd_xCu_y/C catalyst. The metal-support interactions between Pd and WC may be the explanation of the observation that PWA increases BE[33]. Therefore, the synergistic effects of Cu alloying and PWA modification give rise to weaker adsorption of intermediates on the Pd catalysts, which are benefit for catalytic activity enhancement of Pd_xCu_y/PWA-C catalysts.

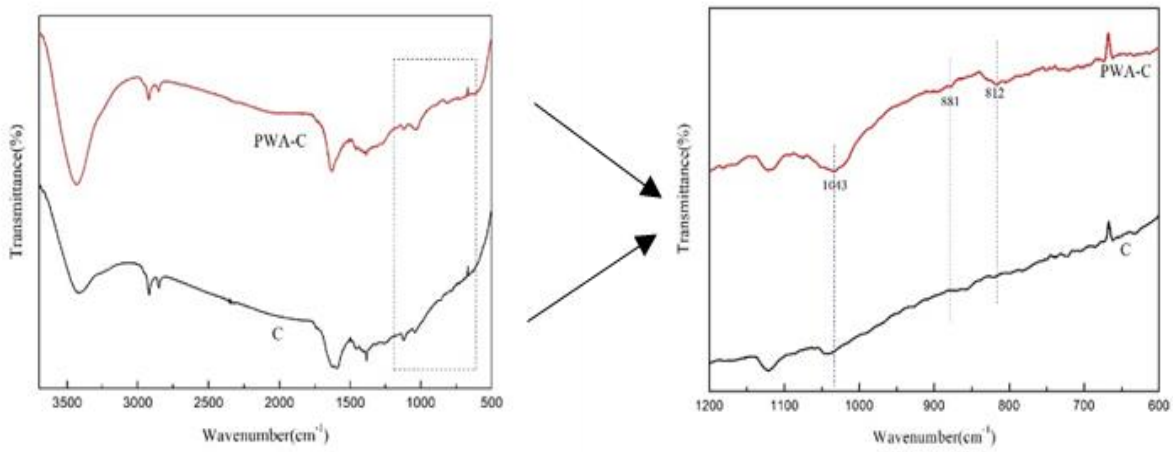

Figure 5. FT-IR spectra of the as-prepared PWA-C and C (Vulcan XC-72).

SEM images and EDS of the Pd_1Cu_2/PWA-C, Pd_1Cu_1/PWA-C, Pd_2Cu_1/PWA-C, Pd_1Cu_2/C, Pd_1Cu_1/C and Pd_2Cu_1/C catalysts are demonstrated in Figure 4. The carbonaceous supports modified by PWA displayed tungsten peaks in their EDS spectra, which confirmed that the catalyst contains tungsten in the Pd_xCu_y/PWA-C. In addition, other elements were all found in the EDS spectrum of corresponding catalysts. It can be seen from the EDS spectra that Pd_1Cu_2/PWA-C has the highest oxygen content among Pd_xCu_y/PWA-C and Pd_xCu_y/C catalysts, which may be helpful for its anti-poisoning performances.

FT-IR spectroscopy was taken to estimate the chemical structure of PWA-C and Vulcan XC-72, illustrated in Figure 5. The absorption bands located at 812, 881, 1043 cm^{-1} were attributed to three characteristic skeletal vibrations of the kegging oxoanions. These absorption bands can be assigned to the vibrations of ν_{as}(P-O_a-$(W)_3$), ν_{as}(M-O_b-W) and ν_{as}(W-O_c-W) in shared octahedral, respectively. These characteristic bands explained that the heteropoly acid molecules acid was successfully modified on the support. The results are in agreement with Yin[34], Mahjoub[35] and Wang[36]. The characteristic absorption peaks explained that the heteropoly acid molecules acid was successfully modified on the support.

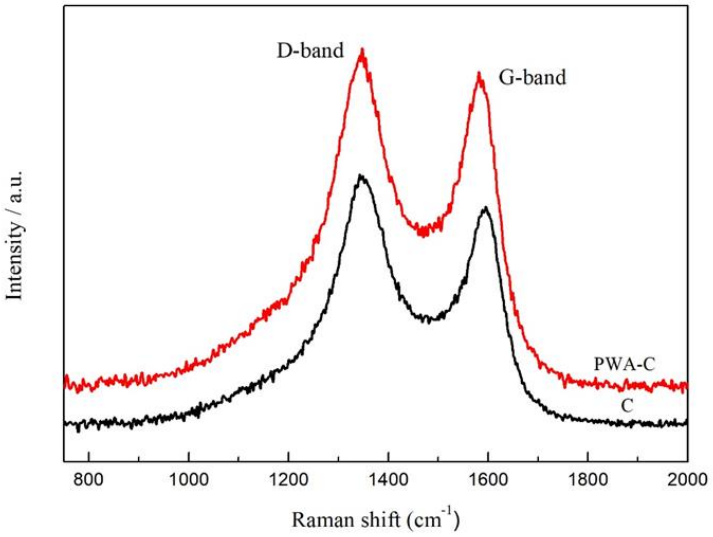

Figure 6. Raman spectra of the as-prepared PWA-C and C (Vulcan XC-72).

In order to investigate the structure and defects of the PWA modified carbon and Vulcan XC-72, Raman spectra were recorded in Figure 6. Raman spectroscopy clearly showed peaks at around 1340 cm^{-1} and 1580 cm^{-1}, corresponding to the D band and G band. The D band was assigned to disordered carbon atoms while G band referred to graphitization degree. It turned out that the I_D/I_G is 1.08 for PWA-C, which is lower than that of Vulcan XC-72 (1.25). The decreasing intensity ratios of I_D/I_G indicated the decreased graphitization degree, and defect density, suggested that the modification of PWA increases the order in the graphitic plane of carbon support, which was in accordance with the previous literature[37, 38].

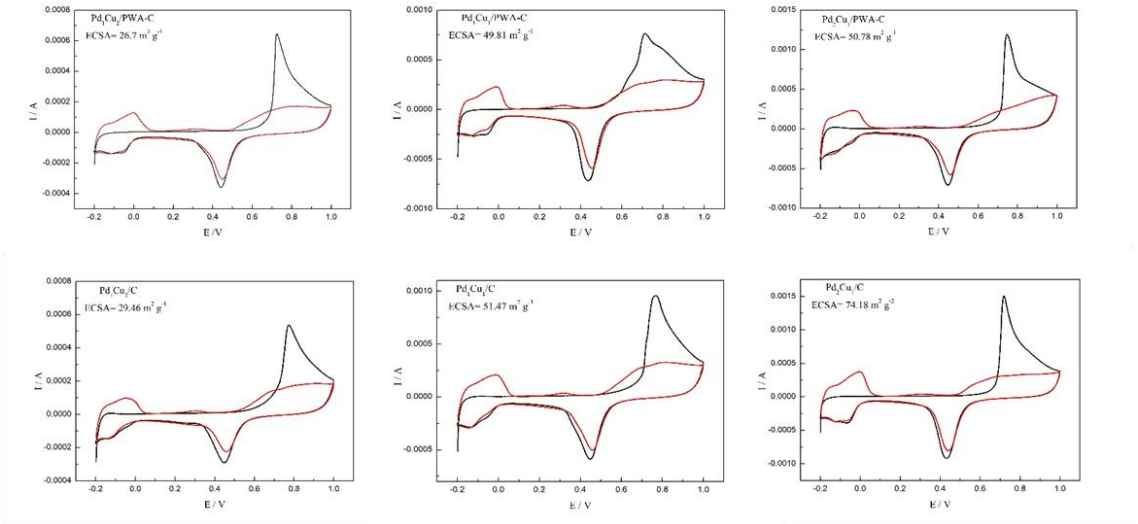

Figure 7. CO-stripping voltammograms of Pd_1Cu_2/C, Pd_1Cu_1/C, Pd_2Cu_1/C, $Pd_1Cu_2/PWA-C$, $Pd_1Cu_1/PWA-C$, $Pd_2Cu_1/PWA-C$ catalysts in 0.5 mol L^{-1} H_2SO_4 solution at a scanning rate of 50 mV s^{-1}.

The CO-stripping voltammograms were used to assess the catalyst performance to resist CO_{ads} poisoning. Figure 7 shows the CO-stripping voltammograms of Pd_xCu_y/PWA-C and Pd_xCu_y/C catalysts, in which the first cycle showed the CO oxidation and the second cycle was the background without CO oxidation. As shown in the figures, both CO stripping peak potential values are lower than the value of 804 mV which was measured for the Pd/C catalyst. The lower potential indicates the weaker Pd-CO bond of the catalysts. As discussed in XPS, the electron transfer effect and the shrunk lattice could weaken the adsorption of some reaction intermediates on Pd surface, as well as enhancing the electrochemical performance[39]. The electrochemical surface area (ECSA) of each catalyst has the following relationship with Q_{CO}, where Q_{CO} is the amount of electricity needed to oxidize CO_{ads}, m is the amount of metal on the electrode, and assuming a value of 420 μc cm^{-2} for the amount of electricity required to oxidize single layer CO_{ads}[40].

$$\mathrm{ECSA}(m^2 g^{-1}) = \frac{Q_{CO}(\mu C)}{420(\mu C\ cm^{-2})} \frac{100}{m(\mu g)} \qquad [1]$$

According to this estimation, the Pd_xCu_y/PWA-C and Pd_xCu_y/C catalysts displayed smaller ECSA with increasing Cu content, and the Pd_xCu_y/PWA-C catalyst has a smaller ECSA than Pd_xCu_y/C catalyst with the same atomic ratio. The CO stripping areas for the Pd_1Cu_2/PWA-C catalyst is about 2.2 times less than that of the Pd/C catalyst. The CO stripping voltammetry results indicate a weak Pd-CO bond strength and a reduction of adsorbed CO on the Pd_xCu_y/PWA-C catalyst surface, especially for Pd_1Cu_2/PWA-C catalyst. The EDS analyses showed that highest oxygen content in the Pd_1Cu_2/PWA-C catalyst also contributes to its anti-CO poisoning.

To further investigate the formic acid oxidation catalytic activities of the samples, the cyclic voltammetry experiments were taken in H_2SO_4/HCOOH aqueous solution. The results of Pd_1Cu_2/C, Pd_1Cu_1/C, Pd_2Cu_1/C and Pd/C catalysts were presented in Figure 8. In the positive scan, formic acid is oxidized and the current is dependent on Pd:Cu atomic. The Pd_1Cu_2 catalyst showed the highest current value as shown in the figure.

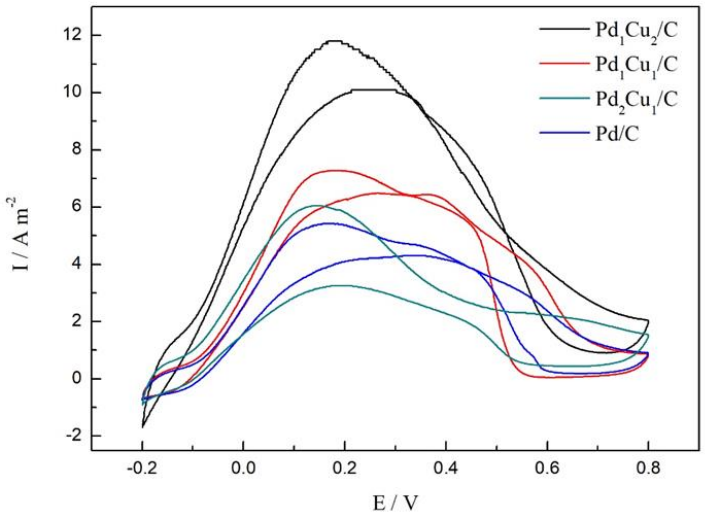

Figure 8. Cyclic Voltammograms of Pd_1Cu_2/C, Pd_1Cu_1/C, Pd_2Cu_1/C and Pd/C catalysts in 0.5 mol L^{-1} HCOOH + 0.5 mol L^{-1} H_2SO_4 solution with a scan rate of 50 mV s^{-1}.

The Pd_xCu_y/C bimetallic catalysts show superior performance compared to the monometallic Pd/C. According the ECSA, the specific oxidative current of Pd_1Cu_2/C, Pd_1Cu_1/C, Pd_2Cu_1/C and Pd/C were calculated as 12.1 A m^{-2}, 7.2 A m^{-2}, 6.0 A m^{-2}, 5.1 A m^{-2}, respectively. Comparing with different Pd/C catalysts, it can be seen there is a 40 mV, 90 mV and 110 mV positive shift in the peak oxidation potential of the Pd_2Cu_1/C, Pd_1Cu_1/C, Pd_1Cu_2/C, respectively. Similar finding were also revealed by Sun[41]. They presented a facile approach to monodispersed CuPd nanoparticles, both the reduction peak and the oxidation peak were shifted. It is believed that Cu alloying is benefit for releasing more active Pd site as discussed above, which improve the electrocatalytic activity of Pd_xCu_y catalysts. Furthermore, the enhancement effect from Cu is strengthened with the increasing Cu content.

Table II. ECSA, peak potential of CO stripping and specific oxidation current of different catalysts**.**

Sample	ECSA (m^2 g^{-1})	Peak potential (mV)	Specific oxidation current (A m^{-2})
Pd/C	52.79	804	7.2
Pd/PWA-C	40.32	753	5.1
Pd_1Cu_2/PWA-C	26.70	711	36.1
Pd_1Cu_1/PWA-C	49.81	714	15.2
Pd_2Cu_1/PWA-C	50.78	747	8.5
Pd_1Cu_2/C	29.46	732	12.1
Pd_1Cu_1/C	51.47	770	7.2
Pd_2Cu_1/C	74.18	773	6.0

In order to study the effects of PWA modification on the catalyst activity, cyclic voltammograms of Pd_xCu_y/PWA-C and Pd_xCu_y/C catalysts with the same atomic ratio are demonstrated in Figure 9. The calculated specific oxidation current of different catalysts is listed in Table II. The specific oxidative current of Pd_1Cu_2/PWA-C, Pd_1Cu_1/PWA-C and Pd_2Cu_1/PWA-C catalysts were calculated as 36.1 A m^{-2}, 15.2 A m^{-2}, 8.5 A m^{-2}, respectively. It was observed that the improvement of electrocatalytic activity by PWA modification with the same Cu content. The higher catalytic effect of PWA-C supported catalyst could be attributed to the interactions between Pd and modified support[33]. It can be found that the Pd_1Cu_2/PWA-C catalytic activity for formic acid oxidation was improved with a factor of 7.07 as compared to Pd/C catalyst. The presence of less electronegativity Cu in PdCu could be better improved for the dehydrogenation reaction, promoting more favorably HCOOH adsorption and dehydrogenation on Pd[41]. Thus, the highest formic acid oxidation was obtained by Pd_1Cu_2/PWA-C catalyst, it can be seen that PdCu alloying and PWA modification existed synergistic effect to promote the formic acid oxidation on Pd_xCu_y/PWA-C catalysts.

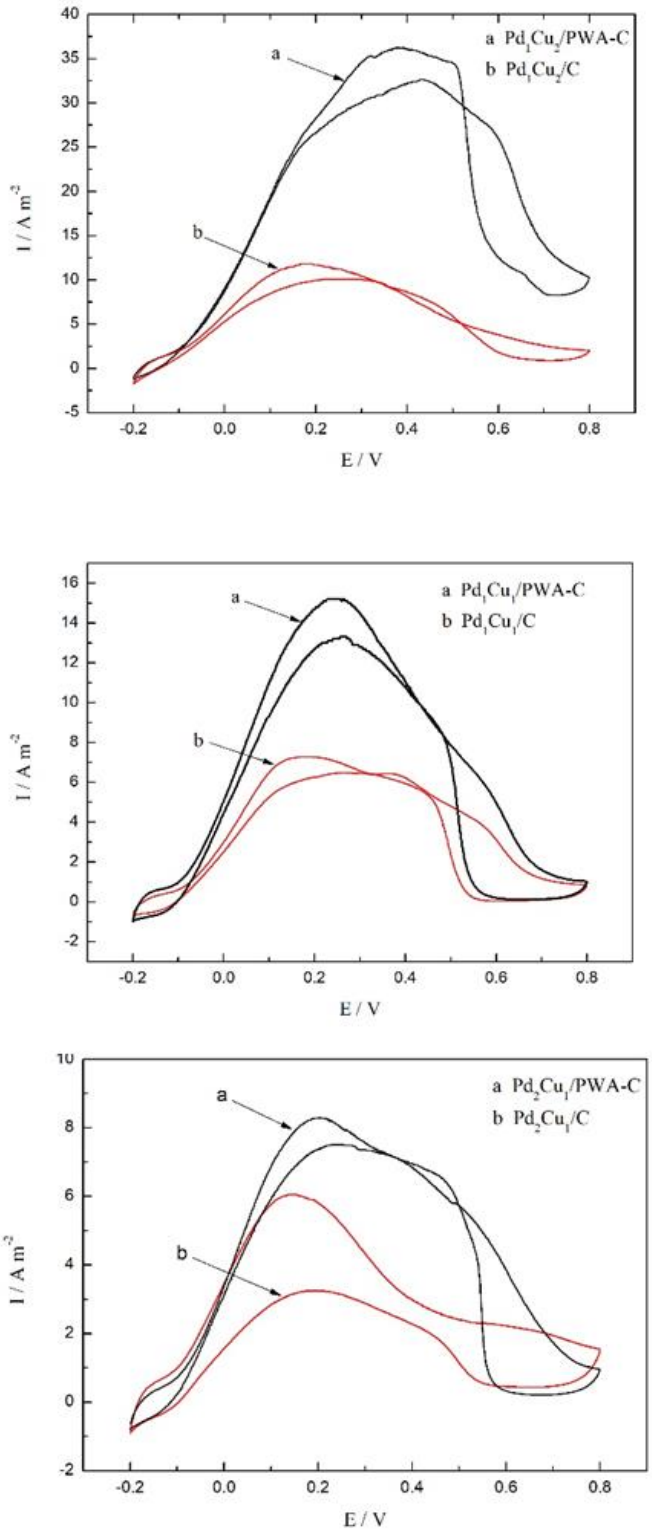

Figure 9. Cyclic Voltammograms of Pd_1Cu_2/C, Pd_1Cu_1/C, Pd_2Cu_1/C, Pd_1Cu_2/PWA-C, Pd_1Cu_1/PWA-C, Pd_2Cu_1/PWA-C electrodes in 0.5 mol L^{-1} HCOOH + 0.5 mol L^{-1} H_2SO_4 solution with a scan rate of 50 mV s^{-1}.

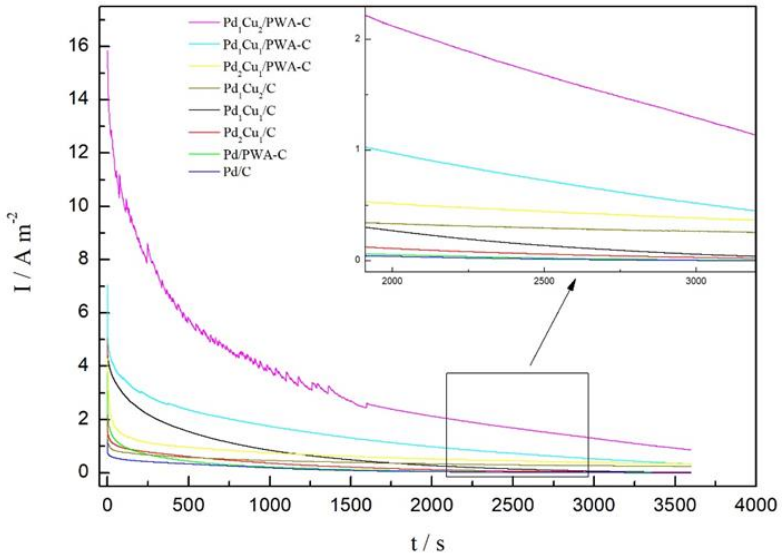

Figure 10. Chronoamperometric curves of Pd_1Cu_2/PWA-C, Pd_1Cu_1/PWA-C, Pd_2Cu_1/PWA-C, Pd_1Cu_2/C, Pd_1Cu_1/C, Pd_2Cu_1/C, Pd/PWA-C and Pd/C catalysts.

The chronoamperometric curves of the catalysts were recorded in the solution 0.5 M H_2SO_4 + 0.5 M HCOOH at 0.1 V and its results were listed in Figure 10. Similar with the results of cyclic voltammetry, the Pd_1Cu_2/PWA-C catalysts possessed remarkable initial current than the other catalysts. As shown in Figure 10, the initial rapid decrease in current is related to the intermediates and toxic substances produced during the formic acid oxidation. The current after 3600 s is 1.3 A m^{-2} for Pd_1Cu_2/PWA-C catalyst, which suggested its superior stability. The current at 3600 s was determined to be 1.30 A m^{-2}, 0.33 A m^{-2}, 0.32 A m^{-2}, 0.23 A m^{-2}, 0.022 A m^{-2}, 0.02 A m^{-2}, 0.015 A m^{-2} and 0.01 A m^{-2} for Pd_1Cu_2/PWA-C, Pd_1Cu_1/PWA-C, Pd_2Cu_1/PWA-C, Pd_1Cu_2/C, Pd_1Cu_1/C, Pd_2Cu_1/C, Pd/PWA-C and Pd/C catalysts, respectively. The Pd_1Cu_2/PWA-C catalyst showed the highest specific activity and stability for the oxidation of formic acid after long term test. The results demonstrated that Cu element and PWA modification can remove CO during the oxidation of formic acid, thus resisting catalyst poisoning, which is in agreement with that of CO-stripping and cyclic voltammetry. The chronoamperometry results are coincided with the previous results[16,18,22].With increasing Cu content, the current of Pd_xCu_y/PWA-C catalysts increase also, which illustrated that the atomic ratio of Pd and Cu also has a great influence on the enhancement of the electrocatalytic stability. Here the Pd_1Cu_2/PWA-C catalyst possesses the best electrocatalytic stability for formic acid oxidation. It is suggested that the Cu alloying and carbon support modified with PWA could ameliorate the electrocatalytic activity and stability of the catalysts.

4. CONCLUSIONS

The PWA modified carbon supported Pd-based bimetallic electrocatalysts for formic acid oxidation were prepared by $NaBH_4$ reduction with different PdCu ratios. The prepared Pd_xCu_y/PWA-C

bimetallic catalyst performed superior electrocatalytic activity and stability than Pd/C catalyst. The optimal results of catalytic performance as to formic acid oxidation was found at Pd_1Cu_2/PWA-C catalyst, whose specific current of formic acid oxidation was improved with a factor of 7.07 as compared to Pd/C catalyst. The lower d-band centre of Pd and the shrunk Pd crystal lattice were developed by Cu alloying. The modification of PWA is benefit for Pd active sites releasing, confirmed by less CO adsorption and better stability of formic acid electro-oxidation. The PWA modification and Cu alloying in Pd nanoparticle play synergistic effects for improvement of the catalytic activity and stability of the electrocatalytic oxidation of formic acid.

ACKNOWLEDGMENTS
This work was supported by the Natural Science Foundation of Hubei Province (Grant No. 2016CFA079) and the financial supports from the Opening Research Fund of Hubei Key Laboratory for Processing and Application of Catalytic Materials (201901403).

References

1. V. Mazumder, M. Chi, M. N. Mankin, Y. Liu, Ã. Metin, D. Sun, K. L. More, and S. Sun, *Nano Lett.,* 12 (2012) 1102.
2. S. Ha, R. Larsen, and R. I. Masel, *J. Power Sources,* 144 (2005) 28.
3. D. Liu, Z. Y. Gao, X. C. Wang, J. Zeng, and Y. M. Li, *Appl. Surf. Sci.,* 426 (2017) 194.
4. Z. Liu, B. Zhao, C. Guo, Y. Sun, Y. Shi, H. Yang, and Z. Li, *J. Colloid Interface Sci.,* 351 (2010) 233.
5. I. M.A. Mohamed, A. S. Yasin, N. A. M. Barakat, S. A. Song, H. E. Lee, and S. S. Kim, *Appl. Surf. Sci.,* 435 (2017) 122.
6. Y. Wang, X. Wang, and C. M. Li, *Appl. Catal. B-Environ.,* 99 (2010) 229.
7. Y. Wang, Y. Zhao, J. Yin, M. C. Liu, Q. Dong, and Y. Q. Su, *Int. J. Hydrogen Energy,* 39 (2014) 1325.
8. X. X. Yang, W. C. Xu, S. Cao, S. L. Zhu, Y. Q. Liang, Z. D. Cui, X. J. Yang, Z. Y. Li, S. L. Wu, A. Inoue, and L. Y. Chen, *Appl. Catal. B-Environ.,* 246 (2019) 156.
9. Z. Yin, Y. N. Zhang, K. Chen, J. Li, W. J. Li, P. Tang, H. B. Zhao, Q. J. Zhu, X. H. Bao, and D. Ma, *Sci.Rep-UK.,* 4 (2014).
10. X. F. Mao, L. C. Yang, J. Yang, J. L. Key, S. Ji, H. Wang, and R. F. Wang, *J. Electrochem. Soc.,* 160 (2013) 219.
11. X. P. Wang, N. Kariuki, J. T. Vaughey, J. Goodpaster, R. Kumar, and D. J. Myers, *J. Electrochem. Soc.,* 155 (2008) 602.
12. M. Kourasi, R. G. A. Wills, A. A. Shah, and F. C. Walsh, *Electrochim. Acta,* 127 (2014) 454.
13. A. R. Motz, M. C. Kuo, G. Bender, B. S. Pivovar, and A. M. Herring, *J. Electrochem. Soc.,* 165 (2018) 1264.
14. Q. F. Tian, Z. W. Zhu, B. Fu, and Y. Li, *J. Electrochem. Soc.,* 165 (2018) 1075.
15. Q. Tian, J. Li, S. Jiang, K. Xia, and Y. Wu, *J. Electrochem. Soc.,* 163 (2016) 139.
16. K. Mandal, D. Bhattacharjee, P. S. Roy, S. K. Bhattacharya, and S. Dasgupta, *Appl. Catal. A-Gen.,* 492 (2015) 100.
17. Z. Zhang, C. Zhang, J. Sun, T. Kou, and C. Zhao, *RSC Adv.,* 2 (2012) 11820.
18. Q. F. Tian, W. Chen, and Y. X. Wu, *J. Electrochem. Soc.,* 162 (2015) 165.
19. B. Richter, H. Kuhlenbeck, H. J. Freund, and P. S. Bagus, *Phys. Rev. Lett.,* 93 (2004) 26805.
20. J. R. Kitchin, J. K. Norskov, M. A. Barteau, and J. G. Chen, *Phys. Rev. Lett.,* 93 (2004) 156801.

21. D. Chen, P. L. Cui, H. Y. He, H. Liu, and J. Yang, *J. Power Sources*, 272 (2014) 152.
22. L. Wang, J.-J. Zhai, K. Jiang, J.-Q. Wang, and W.-B. Cai, *Int. J. Hydrogen Energy,* 40 (2015) 1726.
23. C. J. Corcoran, H. Tavassol, M. A. Rigsby, P. S. Bagus, and A. Wieckowski, *J. Power Sources,* 195 (2010) 7857.
24. M. Wakisaka, S. Mitsui, Y. Hirose, K. Kawashima, H. Uchida, and M. Watanabe, *J. Phys. Chem. B.,* 110 (2006) 23489.
25. C. Q. Sun, Y. Wang, Y. G. Nie, B. R. Mehta, M. Khanuja, S. M. Shivaprasad, Y. Sun, J. S. Pan, L. K. Pan, and Z. Sun, *Phys. Chem. Chem. Phys.*, 12 (2010) 3131.
26. W. J. Zhou and J. Y. Lee, *J. Phys. Chem. C.*, 112 (2008) 3789.
27. J. J. Mao, Y. X. Liu, Z. Chen, D. S. Wang, and Y. D. Li, *Chem. Commun.*, 50 (2014) 4588.
28. H. M. Mao, L. L. Wang, P. P. Zhu, Q. J. Xu, and Q. X. Li, *Int. J. Hydrogen Energy,* 39 (2014) 17583.
29. L. A. Kibler, A. M. El-Aziz, R. Hoyer, and D. M. Kolb, *Angew. Chem. Int. Edit.,* 44 (2005) 2080.
30. M. Ren, Y. Zhou, F. Tao, Z. Zou, D. L. Akins, and H. Yang, *J. Phys. Chem. C.*, 118 (2014) 12669.
31. J. K. Norskov, T. Bligaard, J. Rossmeisl, and C. H. Christensen, *Nat. Chem.*, 1 (2009) 37.
32. D. Kim, J. Resasco, Y. Yu, A. M. Asiri, and P. D. Yang, *Nat. Commun.*, 5 (2014). https://doi.org/10.1038/ncomms5948
33. L. A. Ma, X. A. Zhao, F. Z. Si, C. P. Liu, J. H. Liao, L. A. Liang, and W. Xing, *Electrochim. Acta,* 55 (2010) 9105.
34. H. X. Wu, M. Zhou, Y. X. Qu, H. X. Li, and H. B. Yin, *Chin. J. Chem. Eng.*, 17 (2009) 200.
35. M. Chamack, A. R. Mahjoub, and H. Aghayan, *Chem. Eng. J.*, 255 (2014) 686.
36. R. Wang, G. F. Zhang, and H. X. Zhao, *Catal. Today*, 149 (2010) 117.
37. F. Razmjooei, K. P. Singh, M. Y. Song, and J. S. Yu, *Carbon,* 78 (2014) 257.
38. I. Holclajtner-Antunović, S. Uskoković-Marković, A. Popa, A. Jevremović, B. Nedić Vasiljević, M. Milojević-Rakić, and D. Bajuk-Bogdanović, *React. Kinet. Mech.Cat.*, 128 (2019) 121.
39. F. Gao and D. W. Goodman, *Chem. Soc. Rev.*, 41 (2012) 8009.
40. X. Zhao, J. Zhu, L. Liang, C. Liu, J. Liao, and W. Xing, *J. Power Sources*, 210 (2012) 392.
41. H. Sally Fae, M. G. Adriana, G. Shaojun, H. Kai, S. Dong, L. Sheng, M. Onder, and S. Shouheng, *Nanoscale*, 6 (2014) 6970.